2024 IEEE/RSJ International Conference on Intelligent Robots and Systems (IROS)
October 14-18, 2024. Abu Dhabi, UAE

Towards Design and Development of a Soft Pressure Sensing Sleeve for Performing Safe Colonoscopic Procedures

Mohammad Rafiee Javazm, Sonika Kiehler, Ozdemir Can Kara, and Farshid Alambeigi .

***Abstract*— In this paper, with the goal of enhancing the safety of current colonoscopic procedures and providing the pressure and location of the contact between the colonoscope and the colon's surface, we propose design and development of a unique Soft Pressure Sensing Sleeve (SPSS). SPSS can seamlessly be integrated with the existing colonoscopic devices and would not change the existing diagnosis workflow. The pressure sensing of SPSS is performed based on the resistance change of a liquid metal (i.e., Gallium) embedded into several micro-channels located within SPSS's deformable sleeve when it interacts with the colon surface. To demonstrate functionality of the SPSS, without loss of generality, in this paper, we designed and fabricated a SPSS with 4 sensing regions. We also proposed and experimentally evaluated an empirical calibration function for this sensor. Results demonstrate high accuracy (RMSE=2.45 and mean absolute error $< 3\%$) of the proposed calibration function compared with the evaluation experiments.**

I. INTRODUCTION

The global incidence of colorectal cancer (CRC) has surged significantly in recent years, making it the second most common cause of death from cancer in the United States [1]. Projections based on estimates of population growth and aging indicate that by 2040, CRC cases are expected to rise to 3.2 million [2]. Colonoscopies have long been recognized as the gold standard and a widely practiced method for the screening and diagnosis of CRC. Nevertheless, existing colonoscopes possess limited maneuverability and lack of tactile sensory feedback, which complicates the control of the instrument, makes navigation difficult, and often results in incomplete colonoscopic procedures [3]. Another significant factor influencing the procedure is the force exerted by the surgeon during the insertion of the colonoscope, which can cause significant pain, injury, and discomfort [4]. Appleyard et al. analysed 102 unsuccessful colonoscopic procedures that one-third of the procedures were terminated early because of pain caused by excessive force and looping [5]. Moreover, complications of perforation and bleeding can be related to the application of excessive force to the sigmoid colon [6]. This demands the development of new diagnosis devices to provide accurate and precise interaction force measurement to reduce the complication rate and increase the safety of the procedures.

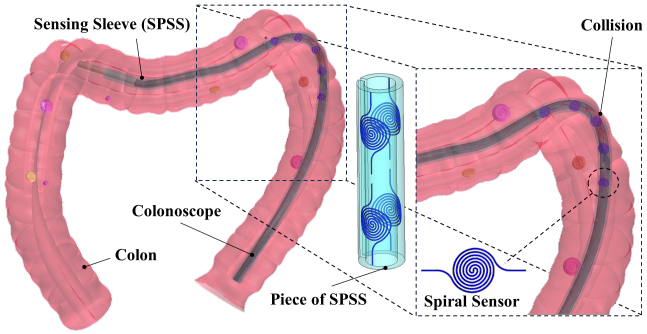

Fig. 1. Conceptual illustration of integrating SPSS with a colonoscope for directly measuring the interaction pressure and detecting the contact location during the colonoscopy procedure.

To address the above-mentioned critical needs in colonoscopic diagnosis, several endoscopic tools with embedded flexible sensors have been developed and reported in the literature. For example, McCandless et al. [7] suggested using a soft robotic sleeve to enhance navigational safety throughout the colonoscopy procedure. This design includes soft and embedded optical sensors and actuators, capable of sensing the contact force between the scope and the colon wall. However, their proposed sleeve can only detect contact along the embedded sensing channels and unable to detect surfaces contacts and areas not covered by the sensors' embedded linear channels. In other words, this makes the proposed sensor line-sensitive (and not surface-sensitive). Furthermore, the minimum detectable force in their study is quite high, which may limit its sensitivity in detecting subtle interactions during colonoscopies procedure. In another effort, Davidson et al. [8] outfitted the insertion tube of an endoscope with an array of pressure sensors to measure the real-time pressure exerted between the endoscope tube and the inner surface during an endoscopic procedure. Naghibi et al. [9] also introduced a soft force sensing module designed to attach around the endoscopic tip to measure both the amplitude and direction of force exerted during endoscopic procedures. However, their approach utilized only strain sensors to detect tip contact and safeguard tissues from unintended or improper bending and perforation. Similarly, in our previous work [10], we developed a soft and inflatable strain-based tactile sensing balloon that captures interaction forces with adjustable sensitivity and load capacity at the tip position. This approach is beneficial for characterizing cancer polyps together with collision detection. Moreover, Watanabe et al. [11] employed a thin fiber to measure the interaction force by leveraging image processing techniques

Research reported in this publication was supported by the National Cancer Institute of the National Institutes of Health under Award Number R21CA280747.

M. R. Javazm, S. Kiehler, O. C. Kara, and F. Alambeigi are with the Walker Department of Mechanical Engineering and Texas Robotics, University of Texas at Austin, TX, USA. Email: mr62958@my.utexas.edu, {sonikakiehler, ozdemirckara}@utexas.edu, and farshid.alambeigi@austin.utexas.edu

on captured images in a scope. However, their approach is limited as it can only identify the interaction force along a small length of the scope. Given that the colonoscope tube typically extends to 1 meter in length, their technique may not perform effectively across such a considerable distance. Recently, Vajpeyi et al. [12] developed a flexible pressure-sensing sleeve for a colonoscope, which spirally covers the insertion tube to measure the contact pressure and avoid extra applied forces to the colon.

In this study and as our main contributions, to collectively address the aforementioned limitations, we propose design, and development of a unique Soft Pressure Sensing Sleeve (SPSS). SPSS can readily be integrated with the existing colonoscopic devices and measure surface interaction pressure along the device to avoid potential injuries during the procedure and enable tactile sensing feedback for clinicians. This pressure sensing is performed based on the resistance change of a liquid metal (i.e., Gallium) embedded into several micro-channels located within SPSS's deformable sleeve when it interacts with the colon's surface. To demonstrate functionality of the SPSS, without loss of generality, in this paper, we focus on the design and a versatile fabrication and calibration procedure for a SPSS with 4 sensing regions together with evaluation of its performance.

II. Methodology

A. Design Requirements of SPSS

Given the flexibility and maneuverability of the insertion tube of the colonoscope within the flexible, stretchable, and tortuous geometry of colon, it is essential for the proposed sensor to seamlessly integrate with the existing devices and accurately measure the contact forces/pressures between the colonoscope and the colon surface. Although the range of interaction forces that may cause colon injury can vary based on the patient's anatomy, a safer maximum interaction force threshold was reported as 13.5 N [13], and maintaining lower force during the procedure is crucial to avoid injury. Thereby, it becomes imperative to consider several design requirements, including (i) Ensuring a sensing sleeve with deformable and soft structure to not change the stiffness of the existing colonoscopes and guarantying a safe interaction with the body, (ii) Minimizing sleeve thickness to avoid substantial changes to the diameter of the colonoscope by considering its outer diameter ranging between 12-15 mm, and the diameter of the colon itself changes between 30 to 80 mm [14], (iii) Enabling surface pressure sensing along the colonoscope; and (iv) Avoiding alterations to the current surgical workflow of colonoscopies, maintaining the established and practiced nature of the intervention.

To satisfy the above-mentioned requirements and inspired by the work proposed by Park et al. [15], [16], we proposed SPSS that relies on the change of resistance of a conductive liquid metal (i.e., gallium) embedded through several spiral-shaped micro-channels located within the elastic sleeve of SPSS. In this study, gallium was chosen as the liquid metal with a melting point of 29 °C instead of Galinstan (a gallium–indium–tin alloy with a melting point of -19 °C) and eutectic gallium–indium (EGaIn with a melting point of 15.5 °C) due to its ability to remain in a liquid state within the body's natural temperature of 37°C, cost-effectiveness, and safety. The properties of these three gallium-based conductive materials are summarized in Table.I. Our method of embedding gallium inside the deformable substrate (i.e., silicon) helps to prevent its oxidation when exposed to air, which reduces its solidification temperature. Of note, the low thermal conductivity of silicon substrate serves to protect the spiral-shaped gallium from the leak and preventing solidification at room temperature.

TABLE I
THE PROPERTIES OF THREE TYPES OF CONDUCTIVE LIQUID METALS BASED ON GALLIUM [17].

Material	Portion (%)			Physical Properties		
	Gallium	Indium	Tin	Melting Point (°C)	Viscosity (cps)	Resistivity (nΩ.m)
Gallium	100	0	0	29.8	2	270
Galinstan	68.5	21.5	10	-19	2.4	289
EGaIn	75.5	24.5	0	15.5	2	294

B. Design and Fabrication of the SPSS

In the fabrication process of the sleeve, two distinct molds have been utilized — one for creating the spiral-shaped gallium micro-channels (shown in Fig. 2f) and another for forming the substrates (shown in Fig. 2k). Fig. 2b illustrates the design of cap and closure molds for the spiral-shaped gallium micro-channels. These molds were fabricated using high-resolution additive manufacturing (Anycubic M5s LCD printer with 19-micron accuracy) using high-clear resin for transparency and visibility. As shown in Fig. 2a-c, to design the spiral-shaped micro-channel mold, several critical considerations have been taken into account, such as incorporating a guide pin for precise mold positioning, holes to fix the mold securely and prevent leakage, and a vent line to facilitate air release during injection and prevent air trapping inside the mold. Inline with the design and size limitations of the colon geometry and recommended by [18], [19] for normal interaction force measurement, a spiral-shaped gallium micro-channel with a circular cross-section was selected, featuring dimensions – detailed in Fig. 2a – including: cross-sectional diameter d_{spiral}= 0.5 mm, maximum coil diameter D_{Coil}= 13.4 mm, and coil distance c = 0.5 mm for optimal size reduction and improved hit localization. Of note, these dimensions can readily be scaled and fabricated thanks to the used 3D printing method. After printing the two sides of the mold (shown in Fig. 2b) and to prepare for the gallium injection, its temperature first was increased using an incubator to reach 40 °C, transitioning it to a liquid state. To prevent solidification during injection, the mold was warmed up to 40 °C after tightening the screws, mitigating the risk of leakage (shown in Fig. 2c). The transparency of the high-clear resin allows for real-time monitoring of the injection process to ensure complete mold filling (shown in Fig. 2d). Subsequently, the mold with injected gallium was placed in a refrigerator to solidify the injected gallium in micro-channel. The solidified spiral-shapes gallium micro-channel was then removed and cleaned from the mold. We made 4

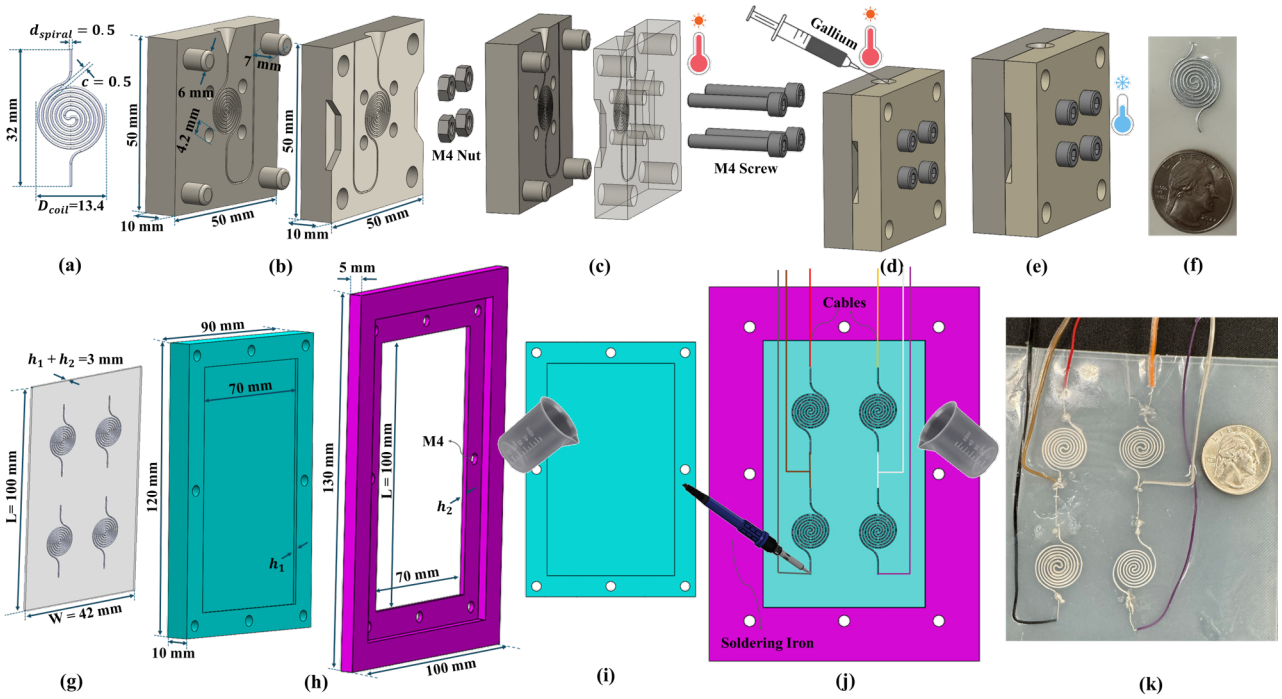

Fig. 2. The entire fabrication procedure for the proposed SPSS components: (a) Design of the spiral channels with critical geometric parameters; (b) Cap and closure molds created with an LCD printer (Anycubic M5s) using high-clear resin for fabrication of micro-channels; (c) Assembly process of the micro-channel mold, including two caps, four M4 screws, and four M4 nuts. The assembled mold is heated to 40 °C using an incubator to prevent gallium solidification during injection; (d) Raising the temperature of gallium to transform it into a liquid state by placing in the incubator set at 40 °C. Subsequently, injecting the liquid gallium into the preheated mold, securely fastened with screws to prevent any potential leakage; (e) Placing the mold in a refrigerator to lower the temperature, facilitating the solidification of gallium, and subsequently removing the formed component; (f) The solidified molded gallium spiral micro channel; (g) Design of the silicon substrate with critical geometric parameters; (h) Two-part mold for fabrication of the silicon substrate; (i) Pouring the first mold using the silicone mixture (Ecoflex 00-30) and allowing it to cure for 4 hours to create the bottom layer of the substrate; (j) Affixing the second part of the mold to the first part, placing the solidified gallium spiral channels on the cured silicone mixture, and connecting conducting wires to their end. Then, pouring and curing the silicone to create the top layer of the substrate; and (k) the fabricated SPSS with 4 embedded gallium spiral channels embedded in the middle of silicon substrate.

spiral-shapes gallium micro-channels using this process to embed them within the silicon substrate and serve as our surface pressure sensors.

As shown in Fig. 2h, to create the deformable substrate and embed the molded 4 spiral-shaped gallium micro-channels in the middle of that, two rectangular molds with different depths were designed to control the thickness of the top and bottom silicon substrate layers. Design parameters (shown in Fig. 2g), such as length (L= 100 mm), width (W= 42 mm), and depths (h_1= 1.25 mm, h_2= 1.75 mm), were carefully chosen considering the aforementioned requirements. Particularly, these dimensions selected based on the size of the utilized colonoscope (i.e., PENTAX EC 3840 L colonoscope) with a 13 mm outer diameter (corresponding to a circumference of 41 mm, based on width W), aiming at minimizing the size added to its outer diameter. To create the bottom layer of silicon substrate, Ecoflex 00-30 (Smooth-On, Inc.), a soft and bio-compatible platinum-cure silicone, was utilized. The silicone mixture, prepared by mixing Part A and Part B in a 1:1 ratio, followed by degassing at a vacuum chamber to eliminate trapped air bubbles. As shown in Fig. 2i, The degassed mixture was then poured into the mold, and any excess material was removed using a flat tool to control its thickness. After curing for approximately 4-5 hours at the room temperature, as illustrated in Fig. 2j, the second part of the mold was fixed to the first layer, and the 4 fabricated spiral channels were precisely placed on the cured silicon layer. Next, the conducting wires were soldered to the two ends of spiral channels as the resistance measurements conductors. The mold was then poured with silicon, similar to the first layer. After curing, the whole substrate was placed in an incubator to increase the temperature and melt the solidified gallium micro-channels inside the silicon substrate. Finally, the flat substrate was removed from the mold. Following the method proposed in [7], we adhered a mesh fabric with a thin layer of silicon (Ecoflex 00-30) to the silicon substrate of SPSS and then sewed the two ends of it to form a cylindrical shape and securely attach the SPSS to the insertion tube of the colonoscope. Fig. 5 shows the attached SPSS to the colonoscope.

III. SPSS Calibration Procedure and Evaluation

A. Calibration Setup

To utilize the SPSS, we first need to calibrate it and correlate the measured resistance of each spiral channel to the contact force and pressure. To this end, we established a calibration strategy to characterize the fabricated sleeve by determining the relationship between the applied forces (F_N)/ pressures(P) and the variable resistance (R) of the spiral-shaped gallium. With this calibration, we can subsequently

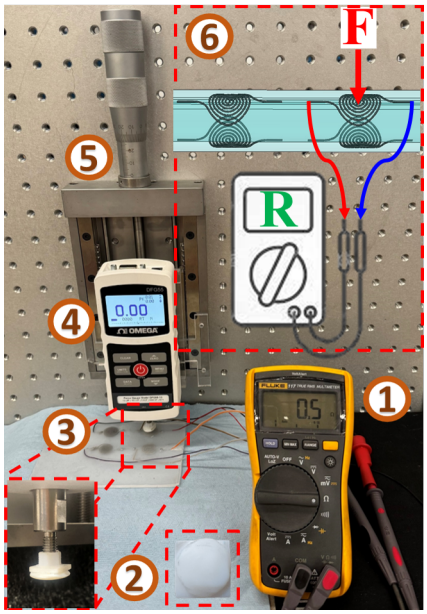

Fig. 3. Experimental Setup: ①- A Fluke Multimeter with 0.1 ohm precision, ②- The flat and rigid contact probe as a contact probe connected to force sensor by thread on the base, ③- The unfolded SPSS with four strain sensor arrays, ④- A Mark-10 Series 5 Digital Force Gauge, ⑤- A M-UMR12.40 Precision Linear Stage, and ⑥- A schematic view of the magnitude and location of contact using an array of spiral sensors.

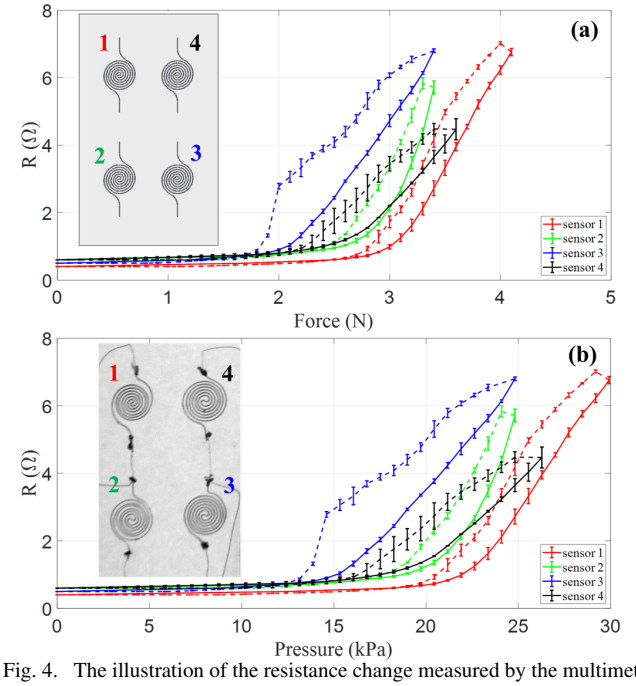

Fig. 4. The illustration of the resistance change measured by the multimeter versus (a) the applied force measured by the force gauge or (b) the calculated pressure using the measured force and interaction area of probe during calibration. We display the mean values and variations across the conducted experiments in both loading (solid line) and unloading (dashed line) cycles. Figure also shows a CAD view of the unfolded SPSS, numbered with different colors corresponding to calibration of each sensor in part (a). Additionally, in part (b), a real image taken with an X-ray machine is provided for inspection of spiral channels.

estimate the normal interaction forces/pressures between the sleeve and the interacting object, such as the surface of the colon in our concept. Fig. 3 illustrates the experimental setup employed for the characterization and calibration of the fabricated SPSS. The illustrated experimental setup in Fig. 3 comprises the unfolded SPSS, a digital force gauge with 0.02 N resolution (Mark-10 Series 5, Mark-10 Corporation) connected to a single-row linear stage with 1 μm precision (M-UMR12.40, Newport) to facilitate accurate movement of the force gauge probe, and a multimeter (Fluke 117 Digital Multimeter) with a resolution of 0.1 Ω to measure resistance changes. Given that the dimensions of the fabricated spiral micro-channels and their location within substrate might slightly vary – that can directly impact their resistance change– independent calibration procedure for each spiral channel was performed. Of note, while the diameter, maximum diameter coil, and gap distance are controlled during fabrication, variations in the length and depth of the spiral-shaped gallium may occur during cutting and pouring, respectively. As shown in Fig. 2i, one end of each spiral channel was electrically connected by a cable in order to reducing number of cable. Consequently, they do not influence each other, allowing for separate calibration.

B. SPSS Calibration Procedure

We used the setup illustrated in Fig. 3 to calibrate each spiral channel in the unfolded configuration. To apply force and measure the resistance of the spiral sensor, a flat and rigid object with an area of 137 mm^2 was employed as a contact probe. The 3D printed object was attached to the force gauge using the threaded connection printed at its base. Given the nonlinear behavior of silicon substrate, utilizing the linear stage mechanism, we conduct tests in incrementally increased (i.e., Loading step) and then decreased (i.e., Unloading step) interaction forces applied to the spiral sensor. This methodology allowed us to comprehend how the sensor's resistance responds to the external forces/pressures. Of note, each spiral channel was measured two times to ensure stability, repeatability, and consistency in calibration.

Fig. 4a illustrates the calibration results, showing the recorded resistances by the multimeter against the interaction forces measured by the force gauge as well as presenting mean values and variations for all spiral channels. Fig. 4b also demonstrated an alternative representation of this calibration, presenting resistance versus the calculated pressures calculated based on dividing the measured interaction forces and the known interaction area.

C. SPSS Loading and Unloading Calibration Functions

In the envisioned colonoscopy procedure using the SPSS, our primary objective is to determine the interaction pressure between each spiral channels embedded within the SPSS and the colon's surface. Therefore, the main goal of this section – using the experimental results depicted in Fig. 4b – is to establish a empirical relationship between the interaction pressure (P) and the variable resistance of each spiral channel (R). Investigation of this figure, we can observe three main features for all spiral sensors: (1) They exhibit a minimum sensing pressure; (2) They have a dead zone region at the beginning; (3) There is a semi-parabolic relationship between the resistance and the interacted pressure in the loading and unloading cycles. Considering these observations, we can

TABLE II

CALIBRATION COEFFICIENTS OF LOADING AND UNLOADING MODELS

Sensor	Loading Coefficients			Unloading Coefficients		
	a_L	h_L	k_L	a_{UL}	h_{UL}	k_{UL}
1	1.15	-6.61	-0.13	-0.92	11.03	5.80
2	0.39	0.91	2.56	-0.49	0.79	2.21
3	1.13	-2.73	-0.09	-1.38	10.54	5.96
4	0.79	0.79	2.07	-2.30	15.15	10.90

model such relationships between resistance and pressure (i.e., $P = \mathcal{G}(R)$) using the *vertex form of a squared-root equation* to obtain an empirical calibration function $\mathcal{G}$ during both the loading and unloading cycles of each sensor. This specific form of the square root equation, expressed as $y = a\sqrt{x-h}+k$, embodies a vertex point (h,k), where, h denotes the horizontal shift along the x-axis, akin to the initial resistance, while k signifies the vertical shift along the y-axis, corresponding to the minimum discernible pressure. Additionally, the parameter a characterizes the steepness of the square root function, analogous to sensitivity. Therefore, using this function, we can determine the coefficients for both loading and unloading cycles through regression analysis, employing the "fit" function in MATLAB. Therefore, for each sensor and using the performed calibration procedure, we can obtain a relationship between the estimated pressure and the measured resistance during both loading and unloading cycles as follows:

$$P^* = \frac{1000}{A_c}\begin{cases} a_L\sqrt{R_L - h_L}+k_L, & \text{Loading} \\ a_{UL}\sqrt{R_{UL}-h_{UL}}+k_{UL}, & \text{Unloading} \end{cases} \quad (1)$$

where R_L, R_{UL}, A_c and P^* represent the resistance in increasing and decreasing steps, contact area, and estimated pressure in kPa, respectively. Also, h_L and h_{UL} denote the initial resistance while h_L and h_{UL} represent to the minimum discernible pressure in the increasing and decreasing steps, respectively. The obtained coefficients of loading and unloading cycles, obtained through the function (1), are summarized in Table.II. Fig. 6 show the form of this empirical function for spiral channel 3 (shown in Fig. 4).

D. Experimental Evaluation of Calibration Function

To assess the estimated pressure P^* obtained using the proposed empirical function (1), we devised an additional experimental setup including the SPSS and a commercial colonoscope (PENTAX EC 3840 L), as illustrated in Fig. 5. For these experiments, we designed and printed a curved contact probe (shown in Fig. 5) with diameter of 20 mm and area of $200mm^2$ matching the curved surface of the SPSS mounted on the colonoscope. For this evaluation experiments, without loss of generality, we selected spiral channel 3 (shown in Fig. 4). We then applied force to this spiral channel using the curved probe to ensure a complete contact surface between the folded SPSS and the probe. Considering the known interaction area A_c of this probe and the measured force using the force gauge, we calculated the actual pressure (P) exerted in the folded sleeve ($P = F_n/A_c$).

Fig. 5. Experimental setup for evaluation of calibration function including the wrapped SPSS with a commercial colonoscope (PENTAX EC 3840 L): ① A fluke multimeter to measure the resistance, ② A curved-shaped contact probe to match the shape of the wrapped SPSS, ③ The wrapped SPSS, ④ A force gauge to measure the interaction force, ⑤ A linear mechanism, ⑥ A schematic view from the folded SPSS attached to the colonoscope under an interaction, and ⑦ A zoomed view of the folded SPSS attached to the colonoscope, positioned next to the scope.

On the other hand, we estimated the pressure using the obtained function (1) along with coefficients obtained from Table II to compare it with the actual pressure. The results from both approaches are depicted in Fig. 6 showing a high accuracy of the proposed empirical model with root mean square error RMSE = 2.45 and the mean absolute error MAE $<3\%$ for pressures more than 14 kPa (i.e., the active sensing region of sensor).

IV. DISCUSSION AND CONCLUSION

The sensor responses depicted in Fig. 4 suggest that each spiral channel exhibit a dead zone at the initial stage, making them unable to detect pressures below the minimum sensing pressure (approximately 10 kPa). Nevertheless, considering the colonoscopy application of SPSS and as reported by Vajpeyi et al. [12], pressures less than $P = 10$ kPa (equivalent to $F_N = 2$ N) are considered safe interactions and therefore are not critical to be measured. Additionally, it is notable that the initial values of each sensor differ due to inherent variations in fabrication and soldering processes, as anticipated. Nevertheless, the overall trends of all sensors, barring sensor 4, exhibit similar patterns, with deviations attributed to uncertainties in the fabrication of the spiral and the soldering of the cable. An X-ray image obtained with the C-Arm X-ray machine (OEC One CFD, GE Healthcare), depicted in Fig. 4b, reveals a significant difference in sensor 4 compared to the other sensors. This variance stems from contact between the coil in the middle section of sensor 4, elucidating the anomalous results observed during the unloading stage. However, given that we calibrate each sensor separately,

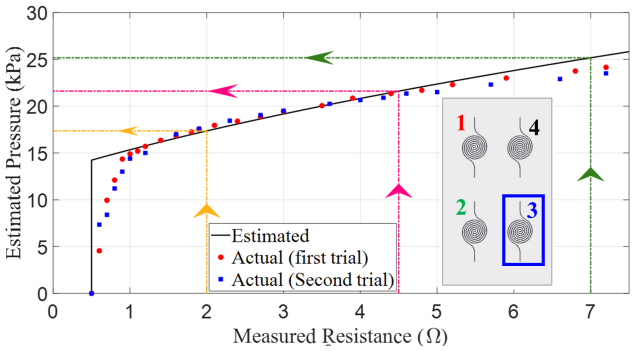

Fig. 6. Comparison of the estimated and actual interaction pressure to validate the empirical calibration model.

this sensor can still measure the interaction pressure with different sensitivity during unloading stage. Also, it is worth noting that although in this study we fabricated a SPSS containing 4 spiral channels (i.e., 4 sensing locations), the proposed fabrication procedure is versatile and can easily be extended to partially or fully cover the whole length of colonoscope.

The comparison of the obtained estimated results with the proposed empirical function (1), clearly demonstrate the high accuracy of the proposed approach. The discrepancy between the initial and end of the modeled function and experimental results can be correlated to the hysteresis of the silicon substrate. Therefore, considering the obtained results, in the envisioned application, we can measure the resistance of each of the spiral-shaped gallium sensors and then directly calculate the contact pressure between each sensor and surface of the sensor. It is worth noting that since we are measuring the resistance change of each spiral channel independently, we are able to also determine the contact locations between the colonoscope and the colon.

To conclude, in this study, with the goal of enhancing the safety of current colonoscopic procedures and providing the pressure and location of the contact between the colonoscope and the colon's surface, we introduced SPSS. SPSS can seamlessly be integrated with the existing colonoscopic devices and diagnosis workflow. To fabricate SPSS, we proposed a unique and versatile fabrication procedure enabling to readily scale the size of the fabricated spiral-shape gallium channels within the silicon substrate of SPSS. We also proposed and evaluated a calibration procedure together with a complementary empirical calibration function for this sensor. Results demonstrate high accuracy (RMSE=2.45 and mean absolute error $< 3\%$) of the proposed calibration function compared with the evaluation experiments.

Despite the promising results shown in this study, in the future, we plan to extend the length and number of sensing locations (i.e., spiral channels) of the fabricated SPSS. We also plan to use the proposed fabrication procedure and fabricate smaller spiral channels and increase their numbers to improve the resolution of contact localization. Moreover, we will conduct user studies to evaluate the performance of our sensor while performing a realistic colonoscopic procedure in colon phantoms.

REFERENCES

[1] R. L. Siegel, N. S. Wagle, A. Cercek, R. A. Smith, and A. Jemal, "Colorectal cancer statistics, 2023," *CA: a cancer journal for clinicians*, vol. 73, no. 3, pp. 233–254, 2023.

[2] Y. Xi and P. Xu, "Global colorectal cancer burden in 2020 and projections to 2040," *Translational Oncology*, vol. 14, no. 10, p. 101174, 2021.

[3] C. W. Iqbal, D. C. Cullinane, H. J. Schiller, M. D. Sawyer, S. P. Zietlow, and D. R. Farley, "Surgical management and outcomes of 165 colonoscopic perforations from a single institution." *Archives of surgery*, vol. 143 7, pp. 701–6; discussion 706–7, 2008. [Online]. Available: https://api.semanticscholar.org/CorpusID:36806838

[4] H. A. Shah, L. F. Paszat, R. Saskin, T. A. Stukel, and L. Rabeneck, "Factors associated with incomplete colonoscopy: a population-based study," *Gastroenterology*, vol. 132, no. 7, pp. 2297–2303, 2007.

[5] M. N. Appleyard, C. A. Mosse, T. N. Mills, G. D. Bell, F. D. Castillo, and C. P. Swain, "The measurement of forces exerted during colonoscopy," *Gastrointestinal endoscopy*, vol. 52, no. 2, pp. 237–240, 2000.

[6] R. Shine, A. Bui, and A. Burgess, "Quality indicators in colonoscopy: an evolving paradigm," *ANZ journal of surgery*, vol. 90, no. 3, pp. 215–221, 2020.

[7] M. McCandless, A. Gerald, A. Carroll, H. Aihara, and S. Russo, "A soft robotic sleeve for safer colonoscopy procedures," *IEEE Robotics and Automation Letters*, vol. 6, pp. 5292–5299, 2021. [Online]. Available: https://api.semanticscholar.org/CorpusID:233877363

[8] T. Davidson, M. Levi, I. Levy, and M. Gilreath, "Endoscope with integrated sensors," Apr. 9 2015, uS Patent App. 14/505,389.

[9] H. Naghibi, M. W. Gifari, W. Hoitzing, J. W. Lageveen, D. M. M. van As, S. Stramigioli, and M. Abayazid, "Development of a multi-level stiffness soft robotic module with force haptic feedback for endoscopic applications*," *2019 International Conference on Robotics and Automation (ICRA)*, pp. 1527–1533, 2019. [Online]. Available: https://api.semanticscholar.org/CorpusID:199004738

[10] M. R. Javazm, O. C. Kara, and F. Alambeigi, "A novel soft and inflatable strain-based tactile sensing balloon for enhanced diagnosis of colorectal cancer polyps via colonoscopy," *IEEE Sensors Journal*, vol. 24, pp. 26 564–26 573, 2024. [Online]. Available: https://api.semanticscholar.org/CorpusID:271254621

[11] T. Watanabe, T. Iwai, Y. Fujihira, L. Wakako, H. Kagawa, and T. Yoneyama, "Force sensor attachable to thin fiberscopes/endoscopes utilizing high elasticity fabric," *Sensors (Basel, Switzerland)*, vol. 14, pp. 5207 – 5220, 2014. [Online]. Available: https://api.semanticscholar.org/CorpusID:6699351

[12] A. Vajpeyi, A. S. Naidu, N. A. Lavdas, J. D. E. Hawel, C. Schlachta, and R. V. Patel, "A novel, flexible, full-length, pressure-sensing sleeve for colonoscopes," *IEEE Sensors Journal*, vol. 24, pp. 2513–2521, 2024. [Online]. Available: https://api.semanticscholar.org/CorpusID:266420986

[13] E. Heijnsdijk, M. Van Der Voort, H. De Visser, J. Dankelman, and D. Gouma, "Inter-and intraindividual variabilities of perforation forces of human and pig bowel tissue," *Surgical Endoscopy and other interventional Techniques*, vol. 17, pp. 1923–1926, 2003.

[14] K. M. Horton, F. M. Corl, and E. K. Fishman, "Ct evaluation of the colon: inflammatory disease," *Radiographics*, vol. 20, no. 2, pp. 399–418, 2000.

[15] Y. Park, B. rong Chen, and R. J. Wood, "Design and fabrication of soft artificial skin using embedded microchannels and liquid conductors," *IEEE Sensors Journal*, vol. 12, pp. 2711–2718, 2012. [Online]. Available: https://api.semanticscholar.org/CorpusID:1350718

[16] Y. Park, C. Majidi, R. K. Kramer, P. Bérard, and R. J. Wood, "Hyperelastic pressure sensing with a liquid-embedded elastomer," *Journal of Micromechanics and Microengineering*, vol. 20, p. 125029, 2010. [Online]. Available: https://api.semanticscholar.org/CorpusID:16256480

[17] S. Cheng and Z. Wu, "Microfluidic electronics." *Lab on a chip*, vol. 12 16, pp. 2782–91, 2012. [Online]. Available: https://api.semanticscholar.org/CorpusID:3103036

[18] B. Shih, J. Mayeda, Z. Huo, C. Christianson, and M. T. Tolley, "3d printed resistive soft sensors," in *2018 IEEE International Conference on Soft Robotics (RoboSoft)*. IEEE, 2018, pp. 152–157.

[19] S. Groß, D. Hidalgo-Carvajal, S. Breimann, N. Stein, A. Ganguly, A. Naceri, and S. Haddadin, "Soft sensing skins for arbitrary objects: An automatic framework," in *2023 IEEE International Conference on Robotics and Automation (ICRA)*. IEEE, 2023, pp. 12 507–12 513.